ISSN: 1410-8917
e-ISSN: 2597-9914

Jurnal Kimia Sains dan Aplikasi 22 (6) (2019): 256–262

Jurnal Kimia Sains dan Aplikasi
Journal of Scientific and Applied Chemistry

Journal homepage: http://ejournal.undip.ac.id/index.php/ksa

The Effect of Cu Ohmic Contact on Photoelectrochemical Property of S-CuO Thin Film Photocathodes

Aziz Amrullah [a], Gunawan [a,*], Nor Basid Adiwibawa Prasetya [a]

[a] Department of Chemistry, Faculty of Science and Mathematics, Diponegoro University, Tembalang, Semarang, Indonesia

*Corresponding Author: gunawan@live.undip.ac.id

https://doi.org/10.14710/jksa.22.6.256-262

Article Info

Article history:

Received: 26th July 2019
Revised: 23rd October 2019
Accepted: 25th October 2019
Online: 30th November 2019

Keywords:
Ohmic Contact; Cyclic Voltammetry; Doped Sulphur

Abstract

The development of semiconductor materials as photocathodes that have excellent performance is significant for the photoelectrochemical reaction of hydrogen evolution. The thin film of sulfur-doped Copper (II) oxide (S-CuO) was successfully synthesized using the cyclic voltammetry method. Investigation of photoelectrochemical properties of S-CuO photocathodes, including current density, onset potential, applied photon to current efficiency (ABPE), and bandgap had been carried out. It was reported that the Cu ohmic contact affected the photoelectrochemical properties and the stability of the thin film. The presence of Cu ohmic contact can improve the performance of S-CuO thin film photocathodes. The S-CuO TU 20 mM thin film has the best response with a current density of -0.923 mA/cm^2, an onset potential of 0.59 V, and ABPE of 0.21%. Stability occurred at pH 7 in 0.2M NaH_2PO_4. The optical analysis showed S-CuO TU 20 mM bandgap of 1.7 eV.

1. Introduction

Research on efficient water splitting into hydrogen and oxygen has become a promising topic for solar energy conversion. Photoelectrochemical (PEC) as a method for the conversion and storage of large-scale solar energy in the form of hydrogen fuel becomes one of the promising technologies to provide clean, cost-effective, and domestically produces energy carriers by utilizing solar radiation[1]. To reduce the cost of converting solar energy into hydrogen, abundance light-absorbing semiconductor materials can be made at low cost and have good photoelectrochemical and stability properties.

Semiconductors used for the water-splitting process must-have criteria including a bandgap of 1.6-2.2 eV, good stability, the bandgap can utilize the solar spectrum (λ> 460 nm) efficiently, potential band edge on the surface must exceed the reduction potential of H_2 and O_2[2]. Some semiconductors such as $CuInSe_2$ (copper indium selenide/CIS), $CuInGaSe_2$(copper indium gallium selenide/CIS), Cu_2ZnSnS_4 (copper zinc tin sulphide/CZTS), and CdTe are well established for use in PEC water splitting applications [3, 4, 5]. Cost considerations and material toxicity cause limitations in the use of the above materials. Copper (II) oxide is considered as a promising candidate because of its abundance in the earth's crust, non-toxic, simple growth process, and high absorption in visible areas[6]. Also, CuO has a bandgap of around 1.2-2.5 eV so that it can absorb significant solar energy[6].

The efficiency of response to light is often a concern of advanced semiconductors. The use of the ohmic contact layer was chosen as one step to increase the efficiency of light absorption. An ohmic contact is defined as contact where there is an uninterrupted transfer from the majority carrier from one material to another and does not limit current. Ohmic contact acts as a reflector, which plays an essential role in increasing cell efficiency[7]. Metals used as ohmic contacts must have low resistance and be thermally stable. Metal with a high work function such as Au, Pd, Se, Ag, Mo, Pt, Cu, can produce ohmic contact for holes and electrostatic barriers for electrons in the hole transporting material (HTM)[8]. However, Mo, Au, Pt, and Pd metals are costly, while Se has a very high work function and at the same time, has very high resistance, and Ag is unstable. Cu is reported to be the optimal ohmic contact in the semiconductor photoresponse [5, 9, 10].

Another step in increasing the semiconductor's response to light absorption and conversion efficiency can be done through doping anions or cations in the semiconductor. Doping anions such as N and S are used to replace oxygen in the oxide lattice, which can shift the valence band upward so that the bandgap is narrowed[11].The development of CuO semiconductors by doping anions and cations has been reported byChiang *et al.* [12] and Ooi *et al.* [13]. The current density at N-CuO is reported at 9.98 x 10^{-5} mA[13], while the current density of Zn-CuO, Co-CuO, Mg-CuO, Ag-CuO, and Fe-CuO are 0.417; 0.77; 0.417; 0.63; and 0.192 mA/cm^2, respectively[12]. Therefore, semiconductor materials with better current density need to be developed. This research developed the S-CuO semiconductor material as a photocathode in water splitting photoelectrochemical cells. In which, the photoelectrochemical properties and their stability at acidic, neutral, and basic pH were studied. The results can be used as a consideration in developing better photocathodes for hydrogen production and its applications on a full scale.

2. Methods

2.1. S-CuO Thin Film Synthesis

Synthesis of S-CuO thin film was carried out in 3 steps, including Cu deposition, S doping, and oxide growth. Cu metal deposition was carried out by electrodeposition method on 2×1 cm^2 glass substrate of fluorine-doped tin oxide/FTO (Sigma Aldrich). The FTO was ultrasonically cleaned in isopropyl alcohol/IPA (Merck, 99.8%) before used. After drying with nitrogen gas, the glass substrate was attached as a working electrode in the electrochemical cell. The electrolyte solution for Cu deposition consisted of 50 mM $CuSO_4.5H_2O$ (Merck, 2,284 g/cm^3), 150 mM $C_6H_5Na_3O_7.2H_2O$ (Merck, 720 g/L), and 242 mM $C_6H_6O_7.H_2O$ (Merck, 1.54g/cm^3). The solution was adjusted to pH 2.5 using 1M H_2SO_4 (Merck, 98%). The constant current of -3 mA/cm^2 was used for Cu deposition for 3600 seconds. Electrodeposition was carried out in three electrodes with FTO as a working electrode, Pt electrode as a counter electrode, and Ag/AgCl as a reference electrode using a Potentiostat (Electrochemical Workstation CorrTest CS Studio 150) instrument in galvanostatic mode.

Sulfur doping was carried out in a cyclic voltammetry (CV) mode using the Potentiostat (Electrochemical Workstation CorrTest CS Studio 150) instrument for 20 cycles. Cu metal deposited on the FTO was used as a working electrode. The CV was carried out at a potential of 0.3 V to -0.6 V (vs Ag/AgCl) containing 0.1 M KCl (Merck, 1.98 g/cm^3) as a supporting electrolyte and 10, 20, and 40 mM $CS(NH_2)_2$ (Merck, 1.405 g/cm^3) as a sulfur precursor. After the cycle was completed, the sulfur-doped Cu deposit was calcined at 600 °C for 3 hours to burn sulfur and grow oxides, so that S-CuO in the FTO substrate was formed.

2.2. Characterization of S-CuO Thin Film

Several characterizations of S-CuO thin film were conducted using XRD, SEM-EDX, DRS UV-Vis and electrochemical measurement. XRD (PANalytical X Pert^3 Powder) was used to determine crystallinity and crystal size. The SEM-EDX (Phenom Pro-X desktop SEM with EDX) used to determine atomic composition. The DRS UV-Vis (Shimadzu UV-2450) was used to determine bandgap, and electrochemistry (linear sweep voltammetry and potentiostatic) to study the photoelectrochemical properties as a photocathode PEC water splitting.

The size of crystals is calculated using the Debye-Scherrer equation (equation 1), where magnitude D is the size of a crystal grain, k is a constant (0.94), λ is the wavelength of X-ray radiation (0.154060 nm), β is the FWHM (Full-Width Half Maximum) value in radians, θ is the Bragg diffraction angle and derived from graph data 2θ on diffractogram.

$$D = \frac{k\lambda}{\beta \cos\theta} \quad (1)$$

$$(\alpha h\upsilon)^n = A(h\upsilon - E_g) \quad (2)$$

Bandgap values were determined by applying the Tauc Plot equation (equation 2) to the transmission spectrum, where α is the absorption coefficient (α = (2,303 x Abs)/d), $h\upsilon$ is energy, A is the proportionality constant, d is the thickness of the thin film, and n varies from 0.5 to 2.0 depending on the nature of the optical transition. For S-CuO thin film, a straight line for $(\alpha h\upsilon)^2$ vs. $h\upsilon$ in the plot (with, n = 2) is used to determine the band direct character of the thin film.

2.3. Measurement of Photoelectrochemical Properties

Measurement of photoelectrochemical properties of photocathodes was evaluated using a potentiostat (Electrochemical Workstation CorrTest CS Studio 150) in linear sweep voltammetry mode with three electrode configurations. The measurement was done by cutting the irradiation of the LED light which was calibrated with a silicon solar cell (measured I_{sc} and V_{oc} under sun light irradiation) with an intensity corresponding to Air Mass/AM 1.5 (100 mW/cm^2) every 10 seconds to the electrode that works below the potential sweep (0.7 to -1.0 V vs Ag/AgCl) with a scanning rate of 10 mV/s in Na_2SO_4 0.1 M at pH 9. Investigation of photoelectrochemical properties included current density, onset potential, and applied bias photon to current efficiency (ABPE).

Measurement of current density was plotted as J-V curve (potential vs. current density) resulting from a linear sweep voltammetry scan. Whereas, the onset potential in each PEC measurement on the photoelectrode for photocathodes, which refers to the Ag/AgCl ($E_{Ag/AgCl}$) electrode converted to E_{RHE} is calculated using equation (3).

$$E_{RHE} = E_{Ag/AgCl} + (0{,}059 \times pH) + 0{,}199 \quad (3)$$

Applied bias photon to current efficiency (ABPE) is determined from the potential current density (J - V) of the photocathode using equation (4). J (mA/cm^2) is the measured current density, V (V vs. RHE) is the bias voltage measured by the RHE scale, V-$V_{H+/H2}$ is the hydrogen equilibrium redox potential (0 V vs. RHE), and P is the photon flux of AM 1.5 sunlight that is 100 mW/cm^2.

$$ABPE\ [\%] = J \times (V\text{-}V_{H+/H2}) \times 100\%/P \quad (4)$$

Semiconductor stability measurements are carried out to determine the resistance of the semiconductor when used in photoelectrochemical water splitting. The stability decrease was determined by equation (5), where the % stability degradation is the magnitude of the decrease in stability expressed in percent, J_o as initial current density, and J_t as final current density.

$$\%\ \text{Stability Degradation} = \frac{Jo - Jt}{Jo} \times 100\% \quad (5)$$

3. Results and Discussion

3.1. Synthesis of S-CuO Thin Film

Cu metal deposition in the FTO was carried out from $CuSO_4.5H_2O$ precursors, citric acid, and sodium citrate according to the procedure used by Gunawan *et al.* [14]. Citric acid and sodium citrate in the solution act as a complexing agent that reduces Cu^{2+} ions[15] and decreases the Cu deposition potential. The electrolyte solution was adjusted to a pH of 2.5 (with the addition of 1M H_2SO_4 solution) according to the Pourbaix diagram. Redox reactions occur in the electrochemical deposition of Cu as in equations (6) to (8).

$$Cu^{2+}{}_{(aq)} + 2e^- \rightarrow Cu^0{}_{(s)} \quad (6)$$

$$H_2O_{(l)} \rightarrow \tfrac{1}{2}O_{2(g)} + 2H^+ + 2e^- \quad (7)$$

$$Cu^{2+} + H_2O \rightarrow Cu^0 + 2H^+ + \tfrac{1}{2}\,O_2 \quad (8)$$

Cu, which had been deposited on the FTO, was doped with sulfur using the Cyclic Voltammetry (CV) method. The potential given was 0.3 V to -0.6 V vs. Ag/AgCl (according to the Cu redox potential window) for 20 cycles with a scanning rate of 10 mV/s. The doping process was carried out from a solution containing thiourea (TU) as a precursor of sulfur and KCl salt as an electrolyte that was adopted from the Navaee procedure[16]. The CV process is shown in Figure 1. The CV curve of Figure 1 produces two peaks consisting of a cathodic peak (E_{pc}) and anodic peak (E_{pa}) with varying peak heights. E_{pc} shows the potential for the reduction of Cu^{2+} to Cu, and E_{pa} shows the potential for the oxidation process of Cu to Cu^{2+}. At CV of 10 mM TU (Figure 1.a) E_{pc1} (1st cycle) occurs at a potential of -0.21 V vs. Ag/AgCl with a high peak while very small E_{pa1} (almost does not appear) occurs at a potential of -0.17 V (vs. Ag/AgCl). Small anodic peaks (hardly appear) indicate that the oxidation process almost did not occur at 10 mM TU. As the CV cycle increases, the E_{pc1} peak shifts towards a more negative potential until the 20th cycle of -0.41 V (vs. Ag/AgCl), and the E_{pa1} peak shifts to a more positive potential of -0.1 V (vs. Ag/AgCl).

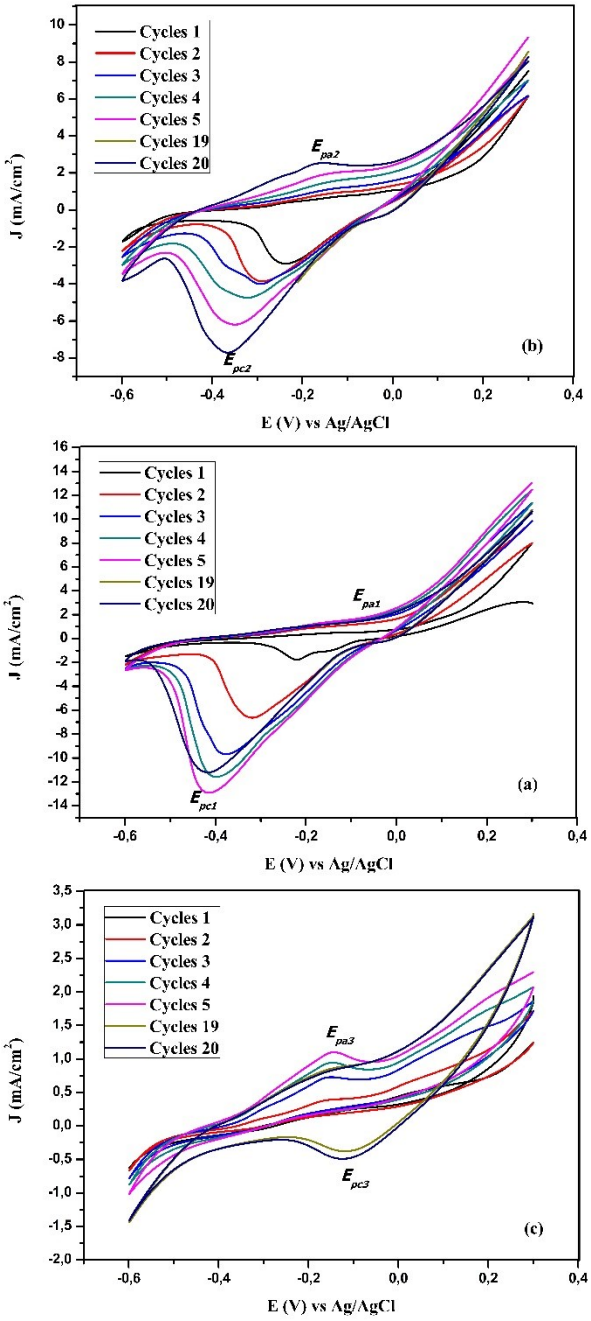

Figure 1. Cyclic Voltammograms obtained through the CV Processes of (a) 10 mM TU, (b) 20 mM TU, and (c) 40 mM TU for Sulphur Doping.

At CV of 20 mM TU (see Figure 1b), the E_{pc2} peak starts at a potential of -0.32 V (vs. Ag/AgCl) while the E_{pa2} peak starts at a potential of -0.15 V (vs. Ag/AgCl). The increase in high peaks indicates stronger interactions with increasing TU concentrations[17]. This confirms the formation of the TU complex with Cu^{2+} ions and the complex is adsorbed on the surface of Cu. The *pa* and *pc* peaks increase with the increase of scan number and scan rate that shows the Cu-TU complex[18] and allows other products to form. Increasing the number of cycles in the CV processes, at a more positive potential, Cu corrodes, and Cu ions are released on the surface of the Cu metal of the working electrode, which is assisted by KCl electrolyte ions. Then, Cu ions are surrounded by TU molecules on the surface of the Cu metal electrode. At a more negative potential occurs the substitution of Cu-TU ions and

adsorbed on the surface of the Cu metal[16]. The CV of 40 mM TU (see Figure 1c) E_{pc3} peak occurs at a potential of -0.16 V (vs. Ag/AgCl) while the E_{pa3} peak occurs at a potential of -0.12 V (vs. Ag/AgCl) with a low peak. Increasing the concentration of TU can also increase corrosion[19] so that the thickness of the thin film gets thinner. The reaction procedure that occurs during the CV process is proposed in equations (9) to (11).

$$Cu_{(s)} \rightarrow Cu_{(s)} \mid Cu^{2+}{}_{(aq)} + 2e^- \quad (9)$$

$$2Cu_{(s)} \mid Cu^{2+} + 4SC(NH_2)_{2\,(aq)} \rightarrow 2Cu \mid CuSNH_2(=NH)_{(s)} + H_2N(HN=)CSSC(=NH)NH_{2(s)} + 2H^+ \quad (10)$$

$$Cu \mid CuSNH_2(=NH)_{\,(s)} + H_2N(HN=)CSSC(=NH)NH_{2(s)} \rightarrow Cu \mid CuO\text{-}S_{(s)} + \textit{Other Products} \quad (11)$$

Initially, there is a portion of the Cu metal electrode, which is oxidized to Cu^{2+} ions on the surface of the Cu. The Cu^{2+} ion is released and surrounded by TU molecules to form the Cu-TU complex and formamidine disulfide (FDS)[20] and other products absorbed on the surface of Cu metal electrodes. Other products that may be formed, such as $Cu_2O_{(s)}$, $Cu_2S_{(s)}$, $Cu_xS_{(s)}$, $NH_{3(g)}$, and other possible products, are formed. After the CV cycle ends, the electrodes were calcined at 600 °C to form oxides. In the calcination process, the component Cu(I) is more dominantly formed from Cu(II) in thin films at low temperatures. However, when the temperature is 500°C, the component of Cu(II) is more dominantly formed than Cu(I)[21], thus allowing oxides from Cu(II) have been formed.

3.2. Characterization of S-CuO Thin Film

XRD analysis (Figure 2) of the S-CuO thin film was carried out in the diffraction angle range (2θ) of 25°-65° with CuKα1 radiation (λ = 1.54060 Å). The peaks that appear on the diffractogram are compared with the standard peaks of the RRUFF (integrated database of Raman spectra, X-ray diffraction, and chemistry data for minerals). The CuO standard, as a comparison, uses RRUFF R120076 data. RRUFF R040017 data is used as a comparison of the peak of the FTO. The RRUFF R050384 data is used as a comparison of Cu_2O peak and RRUFF R061078 as a comparison of Cu peak, respectively.

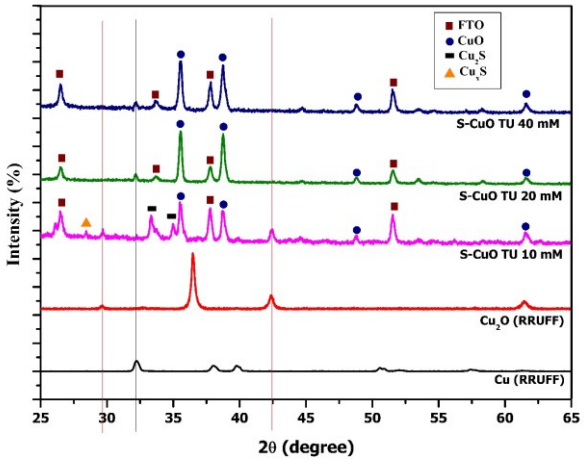

Figure 2. Diffractogram of S-CuO Thin Film, Cu_2O, and Cu.

Figure 2 shows the diffraction pattern of S-CuO thin film prepared by 10 mM TU, the CuO peaks appear at a value of 2θ at 35.53; 38.71; 48.80 and 61.54°. The SnO_2 peaks (FTO) appear at 26.53; 37.76; and 51.50°. Besides, the peaks of Cu_2O are at 2θ of 29.69; 42.48° and the peaks of Cu_2S are at 2θ of 33.31; 34.95° based on RRUFF 120090, and the Cu_xS peak is at 28.43° [16]. On the thin film S-CuO TU 20 mM, the peaks of CuO are at 2θ of 35.57; 38.67; 48.74 and 61.53°. The SnO_2 peaks (FTO) appear at 26.54; 33.70; 37.78; and 51.53°. Whereas the CuO peaks from the 40 mM S-CuO TU thin film appear at 35.57; 38.75; 48.79 and 61.57°. The SnO_2 peaks (FTO) appear at 26.50; 33.67; 37.80; and 51.50°. The S peaks do not appear separately because S has been doped in CuO. S doping on CuO affects the shift of the CuO peak from the CuO standard. In addition, Cu peaks emerge from S-CuO thin films of 20 mM and 40 mM, respectively, at 2θ of 32.19 and 32.21°. This shows that there is a metal layer of Cu under the S-CuO layer, which acts as an ohmic contact. The crystallite size of the thin films S-CuO TU 10 mM, TU 20 mM, and TU 40 mM measured based on the Scherrer equation (equation 1) are 32.08; 38.44; and 40 nm, respectively. Crystallinity influences the charge separation and charge transfer. As the crystalline property of solid increases, the charge separation and charge transfer will be easier (less resistance) so that the resulting dense current will be even greater. The small crystal size can expand the surface of the catalysis so that its performance becomes more effective[22].

The composition of each element contained in the S-CuO thin film semiconductor is known through EDX analysis. EDX analysis results show that sulfur doping on CuO has been successfully carried out. The quantitative composition of the elements S, Cu, and O is presented in Table 1.

UV-Vis DRS characterization was used to determine the band gap energy value of the synthesized thin-film S-CuO semiconductor. Measurements were made at wavelengths of 200-800 nm. Determination of bandgap value (E_g) using the Tauc Plot equation applied to the transmission spectrum obtained from UV-Vis DRS analysis. Measurements were made at S-CuO TU 20 mM, which has better photoelectrochemical properties than other variations. Figure 3 shows the relationship curve $(\alpha h\upsilon)^2$ vs. $h\upsilon$ of the Tauc Plot equation to determine the bandgap value (E_g).

Table 1. Percentage of S-CuO Thin Film Elements Composition Results of EDX Spectrum Analysis.

Thin Film	Composition (%)		
	S	Cu	O
S-CuO TU 10 mM	8.0	52.8	39.2
S-CuO TU 20 mM	0.5	72.1	27.4
S-CuO TU 40 mM	0.3	69.4	30.3

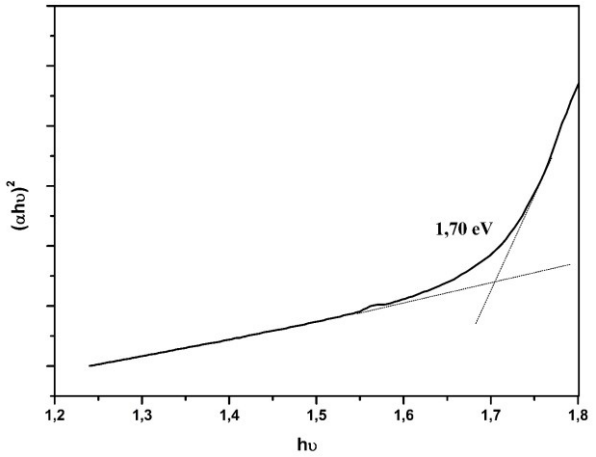

Figure 3. Curve $(\alpha h\upsilon)^2$ vs. $h\upsilon$ Tauc Plot Equation of the Absorbance Value for Determining the S-CuO TU 20 mM Bandgap (E_g).

The bandgap of S-CuO thin films is 1.70 eV, which is smaller than CuO thin films of 1.9 eV[23]. This shows the narrowing of the bandgap due to the influence of doping S. The approach to increasing light response by doping anion can shift the edge of the valence band (vb) upward so that the bandgap energy is reduced[11,24]. From the results of the XRD, EDX, and DRS UV-Vis characterization, the S-CuO thin film and band alignment are illustrated in Figure 4.

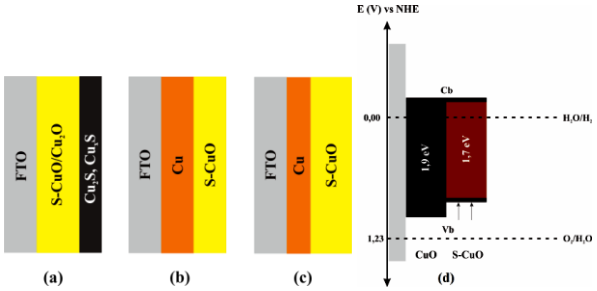

Figure 4. Illustration of S-CuO Thin Film, prepared using (a) TU 10 mM, (b) TU 20 mM, and (c) TU 40 mM from XRD and EDX Characterization, and (d) Band Alignment.

3.3. Effect Cu Ohmic Contact on Photoelectrochemical Properties

Measurement of photoelectrochemical properties was done by cutting irradiation of AM 1.5 (100 mW/cm²) every 10 seconds to the working electrode operating under a sweep potential with a scanning rate of 10 mV/s in 0.1M Na_2SO_4. Measurement of photoelectrochemical properties includes current density, onset potential, and ABPE. Figure 6 shows the results of the measurement of current density and ABPE. From the measurement of current density, it can be determined the onset potential of the photocathode.

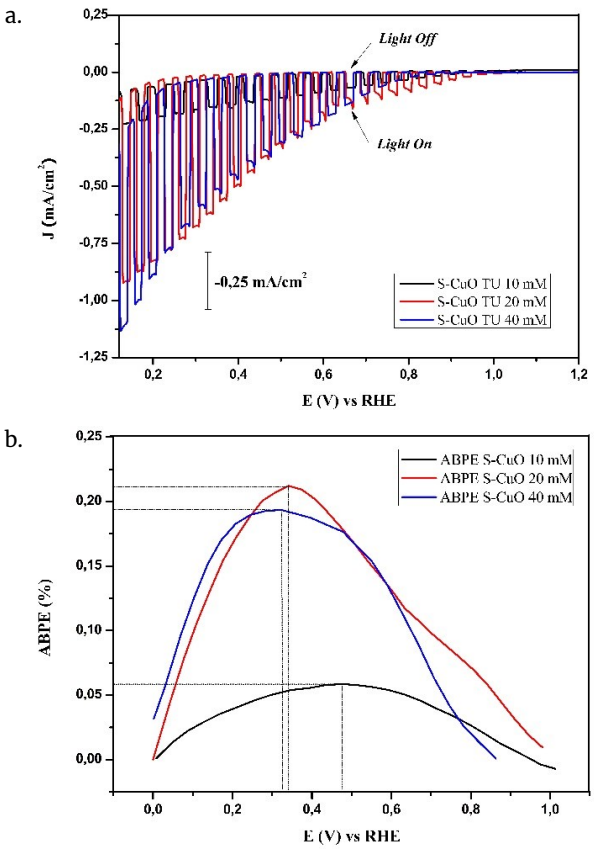

Figure 6. Measurement of S-CuO Thin Film against (a) Current Density, and (b) ABPE measured in 0.1 M Na_2SO_4 by cutting AM 1.5 irradiated light every 10 seconds.

The maximum current density produced by the synthesized S-CuO thin film has a value that varies according to the variation of TU used. The value of the photoelectrochemical property measurement results of S-CuO thin-film semiconductors is further presented in Table 2.

Table 2. Photoelectrochemical Properties of S-CuO Thin Film as measured in 0.1 M Na_2SO_4.

Thin Film	*Photocurrent* (mA/cm²)	*Onset Potential* (V)	ABPE (%)
S-CuO TU 10 mM	-0.123	0.19	0.058
S-CuO TU 20 mM	-0.923	0.59	0.212
S-CuO TU 40 mM	-0.471	0.18	0.193

Table 2 shows the influence of Cu ohmic contact on the photoelectrochemical properties of the thin films. Like Figure 3, the presence of Cu ohmic contact at S-CuOTU 20 mM causes current and potential to increase. While the photoelectrochemical property of S-CuOTU 40 mM decreases again (better than S-CuO TU 10 mM) because the S-CuO film is thinner. The existence of ohmic contact serves to rectify the electric current that flows or passes the electric current. Cu Ohmic contact has small activation energy [9] so that it does not obstruct the transfer of electrons but it can direct and pass an electric current. The electric current at S-CuOTU 10 mM is smaller due to the presence of a layer of impurities Cu_xS and other

products (at top layer) which may be formed during the CV process (see Figure 1a) on the S-CuO TU 10 mM surface thus blocking the absorption of photon energy.

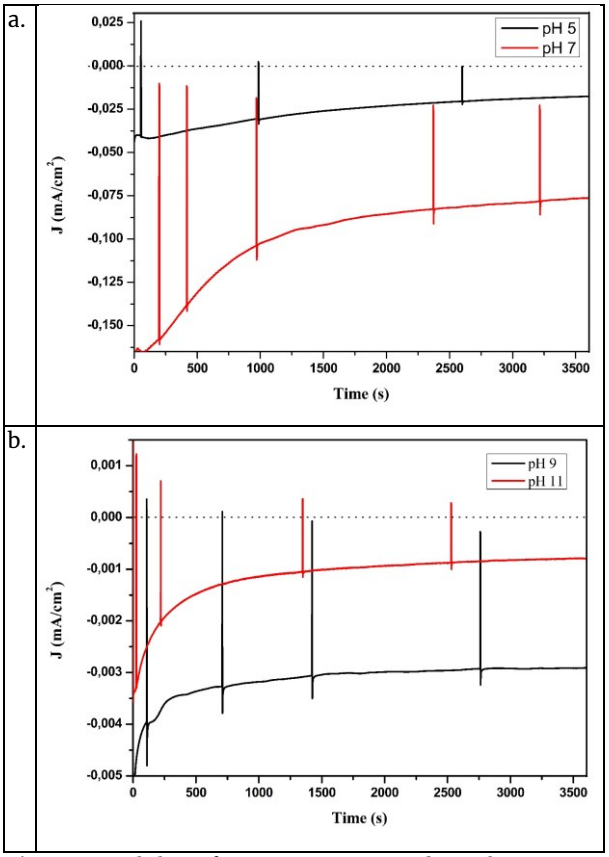

Figure 7. Stability of S-CuO TU 20 mM Thin Film at pH 5, 7, 9, and 11 in 0.2 M NaH_2PO_4 for 3600 seconds.

The current density that appears is observed before the dark current appears at 0 V RHE where the current deflection appears. This shows corrosion in CuO thin film, as expected from the Pourbaix diagram. When a fixed bias of 0 V RHE is applied to the CuO thin film under constant illumination, the current density decreases rapidly to zero in less than 3 minutes, because CuO is converted to Cu metal[25]. Figure 7 shows the stability profile of an S-CuO TU 20 mM photocathode under these measurement conditions. The current density is initially measured at the same potential (0 V vs. Ag/AgCl), then the photocathode measured at pH 9 shows a relatively stable current over time. While in acidic and more alkaline conditions, current density continues to decrease, and the property of photoabsorber tends to disappear. The percentage of degraded thin films of S-CuO TU 10, 20, and 40 mM are 62.23; 60; 33.33; and 77.37%, respectively.

4. Conclusions

Photoelectrochemical properties produced by S-CuO thin film photocathodes with a variation of 20 mM TU had the best photoelectrochemical properties than other variations. A PEC study of water splitting from S-CuO TU 20 mM photocathode revealed that current density, onset potential, and ABPE were affected by Cu ohmic contact. ABPE and maximum onset potential in 0.1M Na_2SO_4 at pH 9 were 0.21% and 0.59 V (RHE), respectively. The stability test showed that the photocathode was stable at pH 9. While under acidic and too alkaline conditions, the photocathode had a rapid current degradation with increasing time (at 0V vs. Ag/AgCl).

References

[1] Zhebo Chen, Todd G. Deutsch, Huyen N. Dinh, Kazunari Domen, Keith Emery, Arnold J. Forman, Nicolas Gaillard, Roxanne Garland, Clemens Heske, Thomas F. Jaramillo, Alan Kleiman-Shwarsctein, Eric Miller, Kazuhiro Takanabe and John Turner, Introduction, in: Z. Chen, H.N. Dinh, E. Miller (Eds.) *Photoelectrochemical Water Splitting: Standards, Experimental Methods, and Protocols*, Springer New York, New York, NY, 2013, pp. 1-5.

[2] Saeid Masudy-Panah, Roozbeh Siavash Moakhar, Chin Sheng Chua, Ajay Kushwaha and Goutam Kumar Dalapati, Stable and Efficient CuO Based Photocathode through Oxygen-Rich Composition and Au–Pd Nanostructure Incorporation for Solar-Hydrogen Production, *ACS Applied Materials & Interfaces*, 9, 33, (2017) 27596-27606 https://doi.org/10.1021/acsami.7b02685

[3] Jin Su, Tsutomu Minegishi and Kazunari Domen, Efficient hydrogen evolution from water using CdTe photocathodes under simulated sunlight, *Journal of Materials Chemistry A*, 5, 25, (2017) 13154-13160 https://doi.org/10.1039/C7TA03761A

[4] Bo Long, Sile Lin, Walter Nsengiyumva and Lingyan Lin, Study of the characteristics of ohmic contact between metal electrodes and Cu_2ZnSnS_4 thin films, *Micro & Nano Letters*, 13, 1, (2018) 27-30 https://doi.org/10.1049/mnl.2017.0274

[5] Kam Hoe Ong, Ramasamy Agileswari, Biancamaria Maniscalco, Panagiota Arnou, Chakrabarty Chandan Kumar, Jake W. Bowers and Marayati Bte Marsadek, Review on Substrate and Molybdenum Back Contact in CIGS Thin Film Solar Cell, *International Journal of Photoenergy*, 2018, Article ID 9106269, (2018) 14 https://doi.org/10.1155/2018/9106269

[6] Saeid Masudy-Panah, Roozbeh Siavash Moakhar, Chin Sheng Chua, Ajay Kushwaha, Ten It Wong and Goutam Kumar Dalapati, Rapid thermal annealing assisted stability and efficiency enhancement in a sputter deposited CuO photocathode, *RSC Advances*, 6, 35, (2016) 29383-29390 https://doi.org/10.1039/C6RA03383K

[7] Rashed Al-Amin, M. F. Pervez, M. N. H. Mia, M. Khalid Hossain, S. M. Rana, N. A. Khan, M. A. S. Haque, H. K. Ghosh and M. Hoq, Influence of Different Metals Back Surface Field on BSF Silicon Solar Cell Performance Deposited by Thermal Evaporation Method, *Advances in Energy and Power*, 5, 3, (2017) 27-31 https://doi.org/10.13189/aep.2017.050301

[8] Najmin Ara Sultana, Md Obidul Islam and Zahid Hasan Mahmood, Utilization of low cost metals as back contact with Perovskite Solar Cell, *Dhaka University Journal of Applied Science & Engineering*, 4, 1, (2017) 35-38

[9] Monisha Chakraborty, Optimum Metal-Semiconductor Contact for Cadmium Sulphide Thin Film, *International Journal of Engineering Research and Applications (IJERA)*, 2, 6, (2012) 793-799

[10] F. Behrouznejad, S. Shahbazi, N. Taghavinia, Hui-Ping Wu and Eric Wei-Guang Diau, A study on utilizing different metals as the back contact of CH3NH3PbI3 perovskite solar cells, *Journal of*

Materials Chemistry A, 4, 35, (2016) 13488-13498 https://doi.org/10.1039/C6TA05938D

[11] Veluru Jagadeesh Babu, Sesha Vempati, Tamer Uyar and Seeram Ramakrishna, Review of one-dimensional and two-dimensional nanostructured materials for hydrogen generation, *Physical Chemistry Chemical Physics*, 17, 5, (2015) 2960-2986 https://doi.org/10.1039/C4CP04245J

[12] Chia-Ying Chiang, Yoon Shin and Sheryl Ehrman, Dopant Effects on Copper Oxide Photoelectrochemical Cell Water Splitting, *Energy Procedia*, 61, (2014) 1799-1802 https://doi.org/10.1016/j.egypro.2014.12.216

[13] Poh Kok Ooi, Mohd Anas Ahmad, Sha Shiong Ng and Mat Johar Abdullah, Characterizations of Nitrogen Doped Cupric Oxide Thin Films Deposited on Different Substrates for Solar Cell Applications, *Advanced Materials Research*, 925, (2014) 469-473 https://doi.org/10.4028/www.scientific.net/AMR.925.469

[14] Gunawan, Abdul Haris, Hendri Widiyandari, Wilman Septina and Shigeru Ikeda, Investigation on Stability of Electroplated-Sulfurized $CuInS_2$-based Photocathode Modified with an In_2S_3 Layer for H_2 Evolution under Various pH Conditions, *Oriental Journal of Chemistry*, 33, 2, (2017) http://dx.doi.org/10.13005/ojc/330202

[15] Sun Min Lee, Shigeru Ikeda, Yasunari Otsuka Takashi Harada and Michio Matsumura, Structural regulation of electrochemically deposited copper layers for fabrication of thin film solar cells with a CuInS2 photoabsorber, *Journal of Non-Crystalline Solids*, 358, 17, (2012) 2424-2427 https://doi.org/10.1016/j.jnoncrysol.2011.12.043

[16] Aso Navaee and Abdollah Salimi, Sulfur doped-copper oxide nanoclusters synthesized through a facile electroplating process assisted by thiourea for selective photoelectrocatalytic reduction of CO2, *Journal of Colloid and Interface Science*, 505, (2017) 241-252 https://doi.org/10.1016/j.jcis.2017.05.103

[17] Farhana Haque, MS Rahman, Etmina Ahmed, PK Bakshi and AA Shaikh, A Cyclic Voltammetric Study of the Redox Reaction of Cu(II) in Presence of Ascorbic Acid in Different pH Media, *Dhaka University Journal of Science*, 61, 2, (2013) 161-166 https://doi.org/10.3329/dujs.v61i2.17064

[18] Maher Alodan and William Smyrl, Effect of thiourea on copper dissolution and deposition, *Electrochimica Acta*, 44, 2, (1998) 299-309 https://doi.org/10.1016/S0013-4686(98)00060-7

[19] Jie Zhao and Guofeng Cui, Study on Adsorption and Complexation Behavior of Thiourea on Copper Surface, *International Journal of Electrochemical Science*, 6, (2011) 4048-4058

[20] A. E. Bolzán, I. B. Wakenge, R. C. V. Piatti, R. C. Salvarezza and A. J. Arvia, The behaviour of copper anodes in aqueous thiourea-containing sulphuric acid solutions. Open circuit potentials and electrochemical kinetics, *Journal of Electroanalytical Chemistry*, 501, 1, (2001) 241-252 https://doi.org/10.1016/S0022-0728(00)00535-0

[21] Sunghoon Park, Soohyun Kim, Sangbo Park and Chongmu Lee, Facile synthesis of CuO nanotubes and their formation mechanism, *Materials Letters*, 138, (2015) 110-112 https://doi.org/10.1016/j.matlet.2014.09.126

[22] Abdul Haris, Gunawan Gunawan, Didik Setiyo Widodo, Rahmad Nuryanto, Retno Ariadi Lusiana and Mei Viantikasari, Synthesis, Characterization of Cu, S doped TiO2 and Its Photocatalytic Activity for Degradation of Remazol Black B, *Jurnal Kimia Sains dan Aplikasi*, 22, 2, (2019) 47-51 https://doi.org/10.14710/jksa.22.2.47-51

[23] Jinyan Pan, Chengfu Yang and Yunlong Gao, Investigations of cuprous oxide and cupric oxide thin films by controlling the deposition atmosphere in the reactive sputtering method, *Sensors and Materials*, 28, 7, (2016) 817-824 https://doi.org/10.18494/SAM.2016.1240

[24] Rufino M Navarro Yerga, M. Consuelo Álvarez Galván, F. del Valle, José A Villoria de la Mano and José L G Fierro, Water Splitting on Semiconductor Catalysts under Visible-Light Irradiation, *ChemSusChem*, 2, 6, (2009) 471-485 https://doi.org/10.1002/cssc.200900018

[25] Wilman Septina, Rajiv Ramanujam Prabhakar, René Wick, Thomas Moehl and S. David Tilley, Stabilized Solar Hydrogen Production with CuO/CdS Heterojunction Thin Film Photocathodes, *Chemistry of Materials*, 29, 4, (2017) 1735-1743 https://doi.org/10.1021/acs.chemmater.6b05248